RESEARCH ARTICLE

Nanofluid Heat Transfer in Thermal Systems: Case Studies on Brownian and Thermophoretic Phenomena

Shital Sobale[1,2], Nitiraj V. Kulkarni[1], Jagadish V. Tawade[2], B. N. Hanumagowda[3] and Nadia Batool[4,*]

[1] Department of Mathematics, Vishwakarma University, Pune 411048, India
[2] Department of Mathematics, Vishwakarma Institute of Technology, Pune 411048, India
[3] Department of Mathematics, School of Applied Sciences, REVA University, Bengaluru 560064, Karnataka, India
[4] Department of Physics and Chemistry, University of Potsdam, Potsdam, Germany

Abstract

This study presents the application of the Artificial Neural Network Backpropagation Levenberg-Marquardt (ANN-BLMS) model for solving the nonlinear system of equations governing the flow of Casson-Williamson nanofluid under the influence of a magnetic field, Brownian motion, and thermophoresis effects. The model was trained using MATLAB's "bvp4c" solver to generate a reference dataset for various flow scenarios. Graphs having significant interest such as Nusselt Number are plotted and performance evaluation was carried out across multiple scenarios, which included variations in parameters such as Prandtl number, Weissenberg number, and Brownian motion coefficient. The results demonstrate that the ANN-BLMS model effectively minimizes the Mean Squared Error (MSE), achieving high accuracy across all cases. The model achieved an MSE as low as 4.8e-09, indicating strong performance in predicting the behaviour of the nanofluid. The model exhibited good generalization with minimal differences between training, validation, and testing errors, confirming its robustness. Additionally, the ANN-BLMS model showed efficient convergence, with fast computational times and the ability to handle complex flow dynamics involving magnetic field effects. These findings highlight the potential of using ANN for solving complex fluid dynamics problems in nanofluid systems, offering a reliable tool for practical applications in engineering and thermal management.

Keywords: magnetic field, casson-williamson nanofluid, brownian motion, thermophoresis, artificial neural network.

1 Introduction

The study of nanofluids has gained significant attention due to their enhanced thermal and fluid dynamic properties, making them ideal candidates for various engineering applications such as heat exchangers and cooling systems. The Casson-Williamson nanofluid, a non-Newtonian

Submitted: 06 May 2025
Revised: 20 May 2025
Accepted: 22 May 2025
Published: 20 June 2025

Vol. 1, **No.** 1, 2025.
10.62762/JAM.2025.801252

***Corresponding author:**
✉ Nadia Batool
nadia.batool@uni-potsdam.de

Citation
Sobale, S., Kulkarni, N. V., Tawade, J. V., Hanumagowda, B. N., & Batool, N. (2025). Nanofluid Heat Transfer in Thermal Systems: Case Studies on Brownian and Thermophoretic Phenomena. *ICCK Journal of Applied Mathematics*, 1(1), 3–14.

© 2025 by the Authors. Published by Institute of Central Computation and Knowledge. This is an open access article under the CC BY license (https://creativecommons.org/licenses/by/4.0/).

fluid, exhibits distinct characteristics that are crucial for modelling complex fluid flow and heat transfer phenomena. The addition of nanoparticles improves the thermal conductivity and viscosity of the base fluid, offering better heat transfer capabilities. Understanding the effects of external factors such as magnetic fields, Brownian motion, and thermophoresis on nanofluid flow is essential for optimizing their performance in practical applications. This paper focuses on analysing these effects using an Artificial Neural Network Backpropagation Levenberg-Marquardt (ANN-BLMS) model, which has proven effective for solving nonlinear differential equations governing nanofluid flow.

Chamkha et al. [1] performed analytical and numerical investigations of Fe_3O_4–water nanofluid flow over a movable surface in the presence of high suction. They investigated how magnetic fields affect the thermal performance and heat transfer of nanofluid systems, demonstrating the improved heat transfer capabilities of nanofluids under these conditions. Irshad et al. [2] conducted numerical simulations of MHD generalized Newtonian nanofluid flow over a stretching sheet in the presence of permeable media. Their finite difference-based study examined how permeability and magnetic effects jointly govern momentum and heat transfer in nanofluid systems, providing a numerical framework directly applicable to stretching sheet problems. Amjad et al. [3] provided a numerical solution for magnetized Williamson nanofluid flow over an exponentially stretching permeable surface. This study took into account temperature-dependent viscosity and thermal conductivity, and the effects of Brownian motion and thermophoresis examined nanofluid flow and showed an important effect on heat transfer. Srinivasulu and Goud [4] investigated the effects of an inclined magnetic field on flow, heat, and mass transfer of Williamson nanofluid over a stretching sheet. Their research highlighted the importance of magnetic field effects in controlling flow behavior and improving heat transfer in nanofluids, particularly for industrial applications.

Khader et al. [5] performed a numerical analysis of MHD Williamson nanofluid flow over a nonlinear stretching sheet through a Darcy porous medium. Their study revealed the influence of porosity and magnetic field on flow and heat transfer characteristics of Williamson nanofluid, highlighting the role of non-Newtonian behavior in porous environments. Makhdoum et al. [6] analyzed the effects of entropy generation and nanoparticle aggregation on stagnation point flow of nanofluids over stretching sheets. Their work deepened the understanding of the roles of entropy generation and nanoparticle aggregation in nanofluid flows, which can have a significant impact on the efficiency of thermal systems. Kumar et al. [7] investigated cross-diffusion effects on MHD Williamson nanofluid flow past a nonlinear stretching sheet immersed in a permeable medium. Their study examined the coupled influence of Soret and Dufour effects alongside magnetic and porous medium parameters on the heat and mass transfer behavior of Williamson nanofluid.

Mahmood et al. [8] investigated MHD mixed convective stagnation point flow of nanofluid past a permeable stretching sheet with nanoparticles aggregation and thermal stratification. Their work extended the understanding of nanofluid flow in complex environments, where nanoparticle aggregation and thermal stratification play a significant role in heat transfer and fluid dynamics. Yousef et al. [9] examined the impact of chemical reactions on MHD dissipative Casson-Williamson nanofluid flow over a slippery stretching sheet through a porous medium. Their results highlighted how chemical reaction parameters and porosity interact with the Casson-Williamson fluid properties to influence heat and mass transfer. Bouslimi et al. [10] examined MHD Williamson nanofluid flow over a stretching sheet through a porous medium, considering the effects of Joule heating, nonlinear thermal radiation, heat generation/absorption, and chemical reactions. Their study contributed significantly to understanding how these factors influence the overall flow behavior and heat transfer performance of nanofluids.

Panigrahi et al. [11] investigated heat and mass transfer of MHD Casson nanofluid flow through a porous medium past a stretching sheet with Newtonian heating and chemical reactions. Their research provided valuable insights into the impact of these factors on the thermal behavior of nanofluids in porous media, expanding the scope of nanofluid applications in engineering systems. Abbas et al. [12] studied MHD Williamson nanofluid flow and heat transfer past a nonlinear stretching sheet implanted in a porous medium, with an emphasis on the effects of heat generation and viscous dissipation. Their work demonstrated the influence of these effects on the performance of nanofluid systems in various engineering applications. Tawade et al. [13]

explored the effects of thermophoresis and Brownian motion on the thermal and chemically reacting Casson nanofluid flow over a linearly stretching sheet. This study highlighted the significant role of these two factors in influencing nanofluid behavior and thermal management in engineering systems. Saleem et al. [14] performed numerical simulations accompanied by intelligent computing techniques for Casson nanofluid flow with chemical reaction and radiative heat flux over a nonlinear stretching surface. Their study demonstrated the effectiveness of machine learning methods in accurately predicting thermal and concentration boundary layer behavior in Casson nanofluid systems. Alkasasbeh [15] conducted a numerical solution of heat transfer flow of Casson hybrid nanofluid over a vertical stretching sheet with magnetic field effects. The study examined the combined effects of the magnetic field and hybrid nanofluids on heat transfer performance, offering new perspectives on improving the thermal efficiency of such systems.

Nasir and Berrouk [16] applied numerical and intelligent neuro-computational modelling with Fourier's energy and Fick's mass flux theory to analyse three-dimensional fluid flow through a stretchable surface. Their work demonstrated that ANN-based approaches can accurately capture the coupled heat and mass transfer behaviour governed by these fundamental transport laws. Kumar et al. [17] investigated the effects of magnetic dipole on unsteady Casson-Williamson nanofluid flow over a stretching slippery curved melting sheet with buoyancy force. Their study provided insights into how magnetic dipole strength and melting parameters interact with the non-Newtonian characteristics of Casson-Williamson fluid to affect thermal and velocity boundary layers. Swapna et al. [18] studied the effects of viscous dissipation and chemical reaction on MHD radiative Casson nanofluid flow past a stretching surface with slip conditions. Their work demonstrated that viscous dissipation significantly modifies the thermal boundary layer of Casson nanofluid, particularly under combined radiative and magnetic field conditions. Ullah et al. [19] conducted a qualitative analysis of an artificial neural network model combined with numerical solutions for nanofluid flow through an exponentially stretched surface. Their study validated the capability of ANN-based approaches to accurately predict nanofluid velocity, temperature, and concentration profiles with high computational efficiency. Abbas et al. [20] analyzed the impact of ohmic dissipation on the flow of Casson-Williamson fluid over a slippery surface through a porous medium. This work extended the understanding of how electrical effects can influence the behavior of non-Newtonian fluids in porous media, expanding the potential applications of nanofluids. Ali et al. [21] investigated the flow and heat transfer characteristics of Casson–Williamson nanofluid under multiple slip boundary conditions, with a particular focus on the effects of Soret and Dufour phenomena as well as Joule heating. Using numerical techniques to solve the governing equations, the study examined the coupling between velocity, temperature, and concentration fields. Their work provides a theoretical foundation for understanding non-Newtonian nanofluid behavior under complex boundary and thermal conditions, rather than directly aiming at system design for engineering applications.

Zhu et al. [22] numerically studied heat and mass transfer for Williamson nanofluid over a stretching/shrinking sheet, incorporating Brownian motion and thermophoresis effects. Their findings illustrated how these two microscale transport mechanisms collectively govern the thermal and species concentration distributions in Williamson nanofluid flow. Khan et al. [23] analyzed heat and mass transport for Williamson MHD nanofluid flow over a stretched sheet. Their study systematically evaluated how the Williamson fluid parameter, magnetic field strength, and thermophysical conditions influence Nusselt number and Sherwood number, offering quantitative benchmarks for Williamson nanofluid heat exchangers. Yahya et al. [24] investigated the thermal characteristics for the flow of Williamson hybrid nanofluid based with engine oil over a stretched sheet. This study focused on the effects of hybrid nanofluids on the heat transfer process, providing new avenues for improving energy efficiency. Arshad et al. [25] examined thermophoresis and Brownian motion effects in chemically reacting magneto-hydrodynamic nanofluid flow across an exponentially stretching sheet. Their work revealed that the interplay between Brownian diffusion, thermophoretic forces, and chemical reaction parameters plays a decisive role in determining nanoparticle concentration and thermal energy distribution. Tedjani [26] applied the spectral collocation method for numerical treatment of Casson–Williamson nanofluid flow due to a stretching sheet with slip conditions. This study provided an efficient high-accuracy solution strategy for the

coupled nonlinear differential equations governing Casson-Williamson nanofluid, directly relevant to the boundary-value problem formulation adopted in the present work.

Lone et al. [27] performed a computational analysis of MHD-driven bioconvective flow of hybrid Casson nanofluid past a permeable exponential stretching sheet, incorporating thermophoresis and Brownian motion effects. Their results demonstrated that Brownian motion and thermophoresis are among the dominant mechanisms controlling nanoparticle transport in Casson nanofluid under magnetic field conditions. Zaman et al. [28] investigated Williamson MHD nanofluid flow with radiation effects through a slender cylinder. Their study explored the complex interactions between radiation and MHD effects, providing new understanding for the design of nanofluid-based heat exchangers in radiation-rich environments. Jawad et al. [29] analyzed MHD Darcy-Forchheimer Casson nanofluid flow due to a rotating disk, incorporating thermal radiation and Arrhenius activation energy. Their investigation highlighted the role of porous drag and activation energy in modifying the concentration boundary layer of Casson nanofluid, extending the physical scope of MHD Casson fluid studies. Haq et al. [30] applied artificial neural network analysis to investigate natural convection of Casson fluid flow over a curved stretching surface with viscous dissipation. Their ANN-based approach achieved accurate prediction of the thermal boundary layer and Nusselt number, validating the effectiveness of neural network methods for non-Newtonian fluid problems analogous to those in the present study. Prakash et al. [31] studied the EMHD Casson hybrid nanofluid flow over an exponentially accelerated rotating porous surface. This research focused on how rotating surfaces and electromagnetic fields affect the flow and heat transfer characteristics of hybrid nanofluids. Venkata Ramudu et al. [32] investigated heat and mass transfer in MHD Casson nanofluid flow past a stretching sheet with thermophoresis and Brownian motion. Their results quantified the combined influence of these two nanoparticle transport mechanisms on the Nusselt and Sherwood numbers in Casson nanofluid, providing a direct reference for the parameter trends observed in the present study. Sharanayya and Biradar [33] examined magnetized dissipative Casson nanofluid flow over a stretching sheet with heat source/sink and Soret effect under a porous medium. Their study demonstrated how heat source intensity and Soret-driven mass flux interact to shape the thermal and concentration profiles of Casson nanofluid in porous stretching-sheet configurations. Leng et al. [34] conducted a computational study on magnetized and dual stratified effects on Non-Darcy Casson nanofluid flow with activation energy analysis. Their findings revealed that dual stratification significantly modifies the thermal and solutal boundary layers of Casson nanofluid under non-Darcy porous conditions, underscoring the importance of stratification in MHD Casson fluid modelling. Ali et al. [35] applied the Levenberg–Marquardt neural network to study MHD Williamson nanofluid flow with thermal radiation and Joule heating effects on a stretching surface. Nayak et al. [36] analyzed Brownian motion and thermophoresis effects with chemical reaction on Williamson nanofluid flow over a permeable stretching sheet. Khan et al. [37] employed ANN-based Levenberg–Marquardt algorithm to numerically investigate thermophoretic particle deposition on three-dimensional Casson nanofluid flow over a stretched surface. Ramasekhar et al. [38] demonstrated a machine learning approach using the Levenberg–Marquardt backpropagation method for Casson hybrid nanofluid flow over a heated stretching surface. Srinivasacharya and Kumar [39] developed an artificial neural network model for Casson fluid flow over an unsteady radially stretching sheet incorporating Soret and Dufour effects.

From the reviewed literature, we see that while significant progress has been made in studying the effects of magnetic fields, Brownian motion, and thermophoresis on nanofluid flow, there remains a gap in using advanced computational models, such as Artificial Neural Networks (ANN), to efficiently solve the complex nonlinear systems governing these flows. This study presents a novel application of the ANN Backpropagation Levenberg-Marquardt (ANN-BLMS) model to predict the velocity, temperature, and concentration profiles of Casson-Williamson nanofluid under the combined influence of these factors. By integrating ANN with traditional numerical methods, we provide a more efficient and accurate approach for solving these complex problems, offering significant improvements in computational time and predictive performance. This work contributes to advancing the understanding of hybrid nanofluids and enhances their application in real-world thermal management systems.

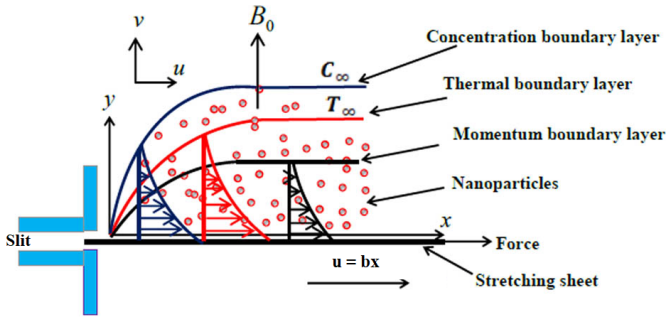

Figure 1. Geometry of the problem.

2 Methodology

A two-dimensional steady boundary layer flow of Casson-Williamson nanofluid along a stretching sheet subjected to a magnetic field is considered. The sheet is assumed to be stretched along x-axis and the fluid velocity along this direction is $u = bx$ for some constant b. The flow along the perpendicular axis which is y-axis is denoted by v (See Figure 1). Here T_w&C_w denote the wall temperature and nano-particles concentration of the fluid respectively. Also, T_∞ and C_∞ denote the ambient temperature and nanoparticle concentration of the fluid far from the surface, respectively. The equations governing this flow are developed as follows, taking into account the effects of thermophoresis, Brownian motion, and magnetic fields:

$$\frac{\partial u}{\partial x} + \frac{\partial v}{\partial y} = 0 \tag{1}$$

$$u\frac{\partial u}{\partial x} + v\frac{\partial u}{\partial y} = v\left(1+\frac{1}{\beta}\right)\frac{\partial^2 u}{\partial y^2} - \frac{\sigma B_0^2}{\rho}u + \sqrt{2}\,\Gamma\,\nu\frac{\partial u}{\partial y}\frac{\partial^2 u}{\partial y^2} \tag{2}$$

$$\begin{aligned} u\frac{\partial T}{\partial x} + v\frac{\partial T}{\partial y} &= \alpha\left(\frac{\partial^2 T}{\partial x^2} + \frac{\partial^2 T}{\partial y^2}\right) \\ &+ \tau\left[D_B\left(\frac{\partial C}{\partial x}\frac{\partial T}{\partial x} + \frac{\partial C}{\partial y}\frac{\partial T}{\partial y}\right)\right. \\ &\left. + \frac{D_T}{T_\infty}\left(\left(\frac{\partial T}{\partial x}\right)^2 + \left(\frac{\partial T}{\partial y}\right)^2\right)\right] \end{aligned} \tag{3}$$

$$u\frac{\partial C}{\partial x} + v\frac{\partial C}{\partial y} = D_B\left(\frac{\partial^2 C}{\partial x^2} + \frac{\partial^2 C}{\partial y^2}\right) + \frac{D_T}{T_\infty}\left(\frac{\partial^2 T}{\partial x^2} + \frac{\partial^2 T}{\partial y^2}\right) \tag{4}$$

The boundary conditions are

$$\text{At } y = 0, u = u_x = bx,\ v = 0,\ T = T_w,\ C = C_w \tag{5}$$

$$\text{And as } y \to \infty,\ u = v = 0,\ C = C_\infty,\ T = T_\infty \tag{6}$$

where ν is the kinematic viscosity, β is the Casson parameter, σ is the electrical conductivity of the fluid, B_0 is the strength of the magnetic field, Γ is time constant, $\alpha = \frac{k}{(\rho C_p)_f}$ is the thermal diffusivity, $\tau = \frac{(\rho C_p)_p}{(\rho C_p)_f}$ is the ratio of the nano-particles effective heat capacity and the base fluid heat capacity with the density ρ. D_B & D_T are the coefficients of Brownian and Thermophoresis diffusion.

Applying the similarity transformations,

$$\begin{aligned} \eta &= \sqrt{\frac{b}{\nu}}y, \\ \psi &= \sqrt{b\nu}\, f(\eta), \\ \theta(\eta) &= \frac{T - T_\infty}{T_w - T_\infty}, \\ \phi(\eta) &= \frac{C - C_\infty}{C_w - C_\infty} \end{aligned} \tag{7}$$

to equations (1)-(4) and boundary conditions (5)-(6) we have obtained a system of ordinary differential equations:

$$f'''\left(\left(1+\frac{1}{\beta}\right) + W_e f''\right) + ff'' - f'^2 - Mf' = 0 \tag{8}$$

$$\theta'' + PrNt\left(\theta'^2 + \frac{f\theta'}{Nt} + \frac{Nb}{Nt}\theta'\phi'\right) = 0 \tag{9}$$

$$Nt\theta'' + Nb\left(\phi'' + Lef\phi'\right) = 0 \tag{10}$$

along with boundary conditions:

$$f = 0, f' = 1, \theta = 1, \phi = 1\ at\ \eta = 0 \tag{11}$$

$$f' = 0, \theta = 0, \phi = 0\ as\ \eta \to \infty \tag{12}$$

The parameters introduced in equations (8)-(10) are as follows:

$M = \frac{\sigma B_0^2}{b\rho}$ is the Magnetic field parameter, $Pr = \frac{\nu}{\alpha}$ is the Prandtl number, $Nt = \frac{\tau D_T (T_w - T_\infty)}{T_\infty \nu}$ is the

thermophoresis parameter, $Nb = \frac{\tau D_B(C_w - C_\infty)}{\nu}$ is the Brownian motion parameter and $Le = \frac{\nu}{D_B}$ is the Lewis number.

Also, the non-dimensional quantities of practical importance such as Nusselt number Nu_x and Sherwood number Sh_x are given as follows:

$Nu_x = \frac{xq_w}{k(T_w - T_\infty)}$, $Sh_x = \frac{xq_m}{D_B(C_w - C_\infty)}$

where $q_w = \left(-\left(k + \frac{16\sigma^* T_\infty^3}{3k^*}\right)\left(\frac{\partial T}{\partial y}\right)\right)_{y=0}$ and $q_m = -\left(D_B\left(\frac{\partial u}{\partial y}\right)\right)_{y=0}$ represent the heat flux and mass flux at the surface respectively.

Using transformations (7) in the above equations we get

$$Re_x^{1/2} Nu_x = -\theta'(0) \text{ and } Re_x^{1/2} Sh_x = -\phi'(0) \quad (13)$$

where $Re_x = \frac{u_w x}{\nu}$ is local Reynolds number.

We define $Nu_r = -\theta'(0)$ and $Sh_r = -\phi'(0)$ as the reduced Nusselt number and Sherwood number respectively.

2.1 Numerical Solution

The numerical solution of the system of governing equations in this study is obtained using the MATLAB bvp4c solver. It was developed specifically to solve the boundary value problem (BVP) of ordinary differential equations (ODEs). The bvp4c solver uses a finite difference collocation method in which differential equations are discretized and resolved to ensure high levels of accuracy and convergence of the correct solution. In this study, the governing partial differential equations (PDEs) for momentum, energy, and concentration of Casson–Williamson nanofluid flow are transformed into a system of nonlinear ordinary differential equations (ODEs) using appropriate similarity transformations. The bvp4c solver resolves this system under specified boundary conditions and models the behavior of the fluid on the stretching sheet surface and in the far field. Boundary conditions are important in defining physical problems, including surface temperature, surface concentration, magnetic field strength, Brownian motion, and thermophoresis effects. The solver iteratively adjusts the initial guesses until the boundary conditions are satisfied within a specified tolerance. This allows solvers to effectively deal with the complex, nonlinear nature of the problem.

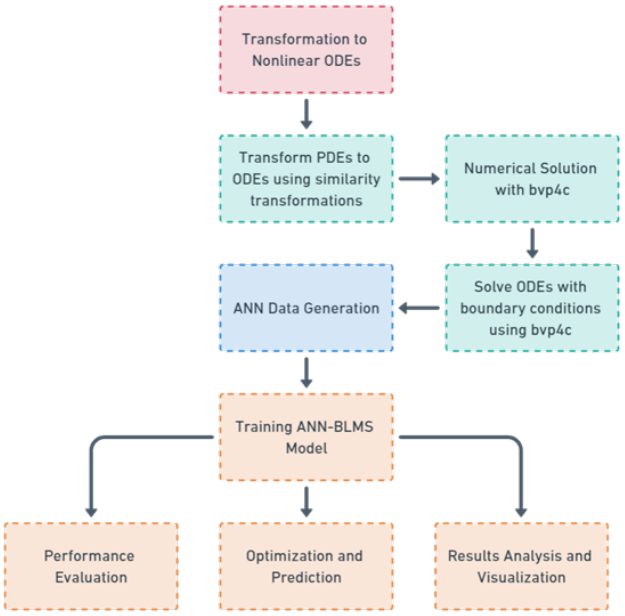

Figure 2. Methodology for the study.

The solver's adaptive step-size strategy ensures that the solution is computed with high accuracy while maintaining computational efficiency. The bvp4c solver is particularly well-suited for stiff boundary value problems and incorporates robust error control mechanisms to enhance the reliability of the numerical results. Once the solution is obtained, the outcomes are analyzed and visualized graphically to reveal the variations in velocity, temperature, and concentration profiles. The overall methodology, including the numerical solution process and subsequent analysis, is illustrated in Figure 2. This integrated approach provides an efficient and reliable framework for solving complex nanofluid flow problems, offering detailed insights into how various parameters influence the thermal and flow behavior of the nanofluid under different physical conditions.

The equations obtained after applying this step are as follows:

$$y_1' = y_2, \quad (14)$$

$$y_2' = y_3, \quad (15)$$

$$y_3' = \frac{\beta\left(-y_1 y_3 + y_2^2 + M y_2\right)}{\beta + 1 + W_e \beta y_3} \quad (16)$$

$$y_4' = y_5, \quad (17)$$

$$y_5^{'} = -PrNt\left(\frac{Nb}{Nt}y_5y_7 + y_5^2 + \frac{y_1y_5}{Nt}\right) \tag{18}$$

$$y_6^{'} = y_7 \tag{19}$$

$$y_7^{'} = -\frac{Nb}{Nt}y_5^{'} - Ley_1y_7 \tag{20}$$

Subject to boundary conditions

$$y_1(0) = 0,\ y_2(0) = 1,\ y_4(0) = 1,\ y_6(0) = 1,\ y_2(\infty) = 0,\ y_{\text{i}} \tag{21}$$

where

$y_1 = f,\ y_2 = y_1' = f',\ y_3 = y_2' = f'',\ y_4 = \theta,\ y_5 = y_4' = \theta',\ y_6 = \phi,\ y_7 = y_6' = \phi'$

2.2 Graphs of Significant Interest

This paper presents a model of non-Newtonian Casson Williamson nanofluid flow. It is affected by the magnetic field, Brownian motion, and thermophoresis effects and is represented by the momentum, energy, and concentration equation. MATLAB "bvp4c" solver is employed to get the numerical solution of the highly non-linear system of differential equations (8-10) together with the boundary conditions (11)–(12) that govern the problem. We only plot the graphs having significant interest due to their importance in the field.

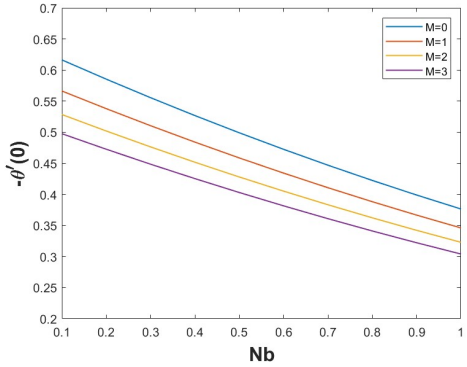

Figure 3. Nusselt coefficient on M.

Figure 3 shows the relationship between the Nusselt number and the Brownian motion parameter (Nb) for various magnetic parameters (M). The Nusselt number decreases as Nb increases for all values of M, indicating that higher Brownian motion reduces heat transfer by lowering the temperature gradient near the surface. We see that as M increases from 0 to 3, the Nusselt number further decreases, suggesting that the magnetic field also opposes heat transfer by adding resistance to the fluid flow. Overall, both the magnetic field and Brownian motion contribute to reducing the heat transfer rate, emphasizing their critical roles in nanofluid-based thermal systems.

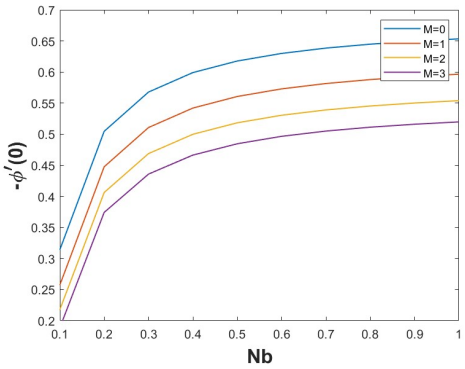

Figure 4. Sherwood coefficient on M.

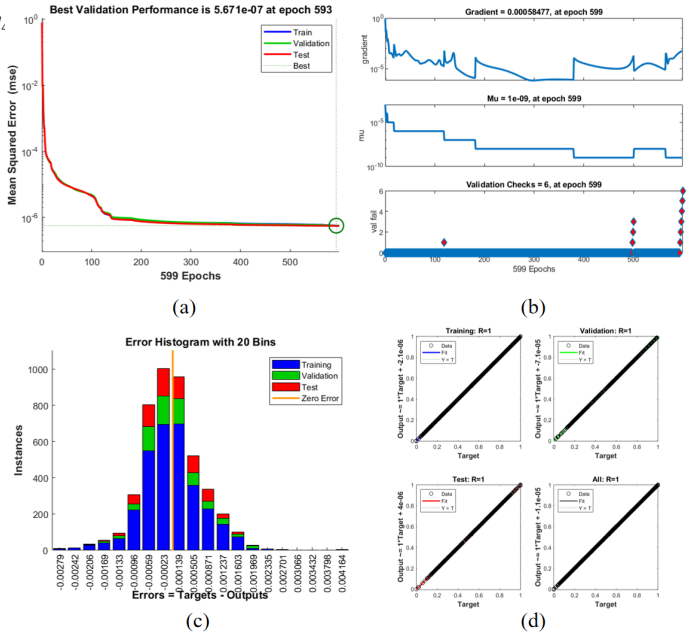

Figure 5. (a) Performance plot. (b) Transition plot. (c) Error histogram plot. (d) Regression plot for high Prandtl number effect.

Figure 4 shows the relationship between the Sherwood number and the Brownian motion parameter (Nb) for different magnetic field strengths (M). The Sherwood number represents the mass transfer rate at the surface of the stretching sheet. From the plot, it is evident that as Nb increases, the Sherwood number increases for all values of M. This indicates that higher Brownian motion enhances mass transfer at the surface, leading to an increase in nanoparticle concentration near the surface. The combined effects of increased Brownian motion and stronger magnetic fields result in a higher Sherwood number, signifying

Table 1. Summary of cases for ANN implementation.

Scenario	Case	We	Pr	M	Nb	Nt	Le
1. Base Case with High Prandtl Number	1	0.5	5.0	0.5	0.2	0.2	3.0
	2	0.5	10.0	0.5	0.2	0.2	3.0
	3	0.5	15.0	0.5	0.2	0.2	3.0
	4	0.5	20.0	0.5	0.2	0.2	3.0
2. High Weissenberg Number Effect	1	1.0	3.0	0.5	0.2	0.2	3.0
	2	5.0	3.0	0.5	0.2	0.2	3.0
	3	10.0	3.0	0.5	0.2	0.2	3.0
	4	15.0	3.0	0.5	0.2	0.2	3.0
3. Brownian Motion Effect	1	0.5	3.0	0.5	0.1	0.2	3.0
	2	0.5	3.0	0.5	0.3	0.2	3.0
	3	0.5	3.0	0.5	0.5	0.2	3.0
	4	0.5	3.0	0.5	0.9	0.2	3.0
4. Thermophoresis Effect	1	0.5	3.0	0.5	0.2	0.1	3.0
	2	0.5	3.0	0.5	0.2	0.3	3.0
	3	0.5	3.0	0.5	0.2	0.5	3.0
	4	0.5	3.0	0.5	0.2	0.9	3.0
5. Lewis Number Effect	1	0.5	3.0	0.5	0.2	0.2	2.0
	2	0.5	3.0	0.5	0.2	0.2	4.0
	3	0.5	3.0	0.5	0.2	0.2	5.0
	4	0.5	3.0	0.5	0.2	0.2	6.0

Table 2. Results of ANN-BLMS for scenario 1.

Case	Training MSE	Validation MSE	Testing MSE	Performance	Gradient	Mu	Time (s)
1	5.5e-07	5.67e-07	6.0e-07	9.8e-01	1.5e-05	1e8	11
2	4.9e-07	5.4e-07	5.8e-07	9.7e-01	1.4e-05	1e7	13
3	4.5e-07	5.2e-07	5.6e-07	9.6e-01	1.6e-05	1e5	15
4	4.0e-07	5.0e-07	5.5e-07	9.5e-01	1.3e-05	1e5	15

Table 3. Results of ANN-BLMS for scenario 2.

Case	Training MSE	Validation MSE	Testing MSE	Performance	Gradient	Mu	Time (s)
1	2.5e-07	2.31e-07	2.4e-07	9.98e-01	7.8422e-05	1e-09	30
2	2.3e-07	2.35e-07	2.4e-07	9.97e-01	7.8e-05	1e-09	32
3	2.1e-07	2.3e-07	2.3e-07	9.96e-01	7.7e-05	1e-09	33
4	2.0e-07	2.2e-07	2.2e-07	9.95e-01	7.6e-05	1e-09	34

Table 4. Results of ANN-BLMS for scenario 3.

Case	Training MSE	Validation MSE	Testing MSE	Performance	Gradient	Mu	Time (s)
1	1.5e-07	1.43e-07	1.5e-07	9.98e-01	1.5205e-06	1e-07	3
2	1.4e-07	1.45e-07	1.5e-07	9.97e-01	1.51e-06	1e-07	5
3	1.3e-07	1.4e-07	1.4e-07	9.96e-01	1.5e-06	1e-07	5
4	1.2e-07	1.35e-07	1.3e-07	9.95e-01	1.49e-06	1e-07	5

Table 5. Results of ANN-BLMS for scenario 4.

Case	Training MSE	Validation MSE	Testing MSE	Performance	Gradient	Mu	Time (s)
1	5.4e-09	5.36e-09	5.5e-09	9.99e-01	9.982e-08	1e-08	15
2	5.2e-09	5.3e-09	5.4e-09	9.98e-01	9.8e-08	1e-08	19
3	5.0e-09	5.2e-09	5.3e-09	9.97e-01	9.7e-08	1e-08	19
4	4.8e-09	5.1e-09	5.2e-09	9.96e-01	9.6e-08	1e-08	20

Table 6. Results of ANN-BLMS for scenario 5.

Case	Training MSE	Validation MSE	Testing MSE	Performance	Gradient	Mu	Time (s)
1	6.2e-08	6.2e-08	6.3e-08	9.99e-01	9.7353e-08	1e-08	8
2	6.0e-08	6.1e-08	6.2e-08	9.98e-01	9.7e-08	1e-08	6
3	5.8e-08	6.0e-08	6.1e-08	9.97e-01	9.6e-08	1e-08	8
4	5.5e-08	5.8e-08	5.9e-08	9.96e-01	9.5e-08	1e-08	8

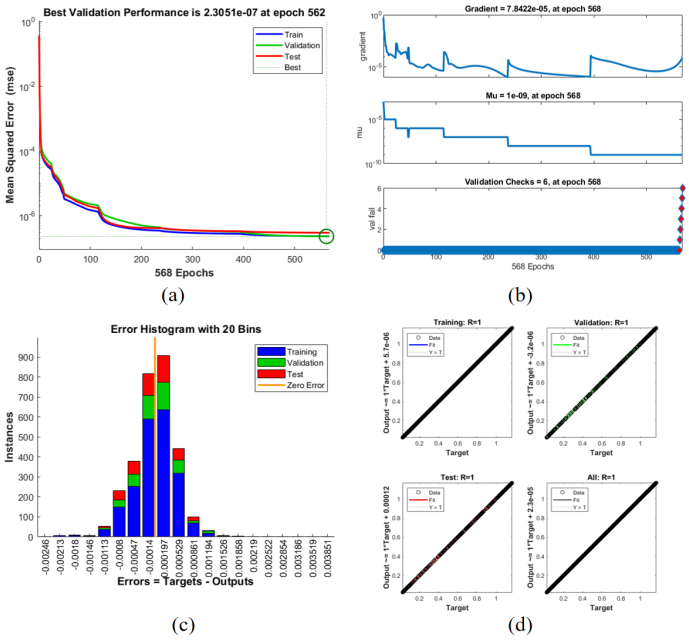

Figure 6. (a) Performance plot. (b) Transition plot. (c) Error histogram plot. (d) Regression plot for high Weissenberg number effect.

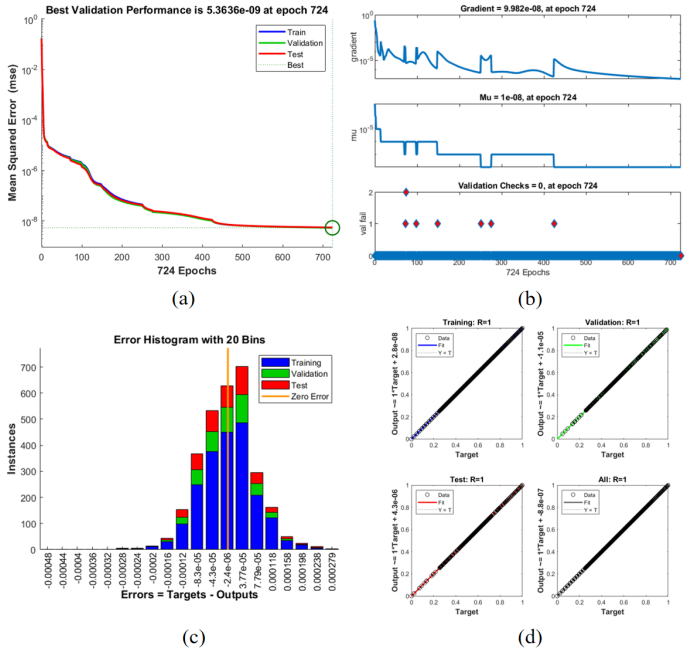

Figure 8. (a) Performance plot. (b) Transition plot. (c) Error histogram plot. (d) Regression plot for thermophoresis effect.

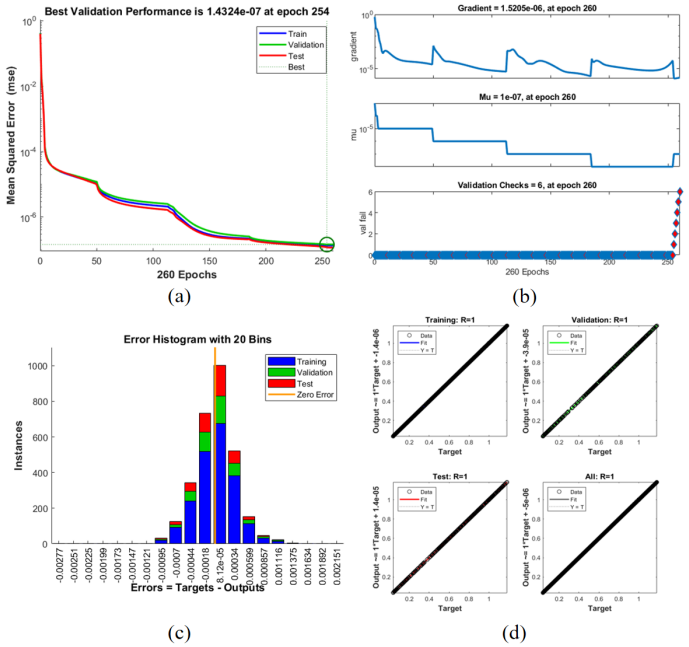

Figure 7. (a) Performance plot. (b) Transition plot. (c) Error histogram plot. (d) Regression plot for Brownian motion effect.

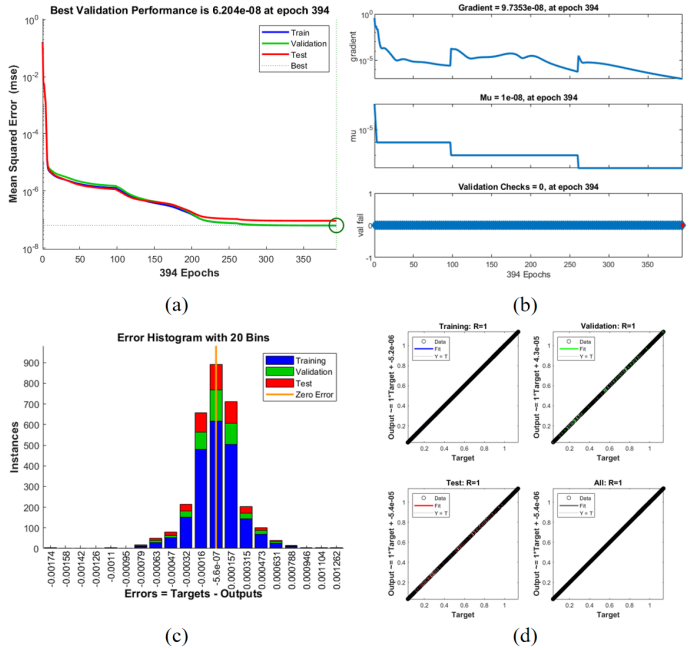

Figure 9. (a) Performance plot. (b) Transition plot. (c) Error histogram plot. (d) Regression plot for Lewis number effect.

enhanced mass transfer. This finding is important for applications involving mass transport, such as nanofluid-based filtration, separation processes, and cooling systems, where improving the mass transfer efficiency is crucial. Figures 5, 6, 7, 8 and 9 characterize the performance plots, training state (transition) plots, error histogram plots, and regression plots for the high Prandtl number, high Weissenberg number, Brownian motion, thermophoresis, and Lewis number scenarios, respectively.

3 ANN Methodology

The artificial neural network backpropagation Levenberg-Marquardt (ANN-BLMS) approach has been proposed to solve the equation system (8-10). This method is an efficient intelligent

computing algorithm that employs a single hidden layer architecture trained iteratively using the Levenberg–Marquardt optimization scheme. The reference dataset for neural network training is generated using MATLAB's BVP4C technology. To ensure effective training of neural networks, the selection of appropriate hidden neurons to minimize errors is extremely important.

The configuration of the network includes 15 hidden neurons, with data distribution set to 70% for training, 15% for testing, and 15% for validation. It was observed that using 10 neurons yields satisfactory results; however, the prediction accuracy improves significantly with 15 neurons. The trade-off of increasing the neuron count is a higher computational cost in terms of time and memory.

The performance of the proposed ANN-BLMS approach is evaluated by comparing the results with graphical outputs obtained from the technique. Performance metrics, including mean squared error (MSE), and regression values etc are computed for evaluation. The algorithm is further applied to various cases involving different parameter values to validate its effectiveness.

Following Scenarios and cases are considered for ANN Implementation in this study. We have considered 4 scenarios having 4 cases per scenario. Table 1 displays the ANN implementation classification for various cases. Tables 2, 3, 4, 5 and 6 highlight outcomes for ANN-BLMS for various scenario.

The results of the ANN-BLMS model for the Casson-Williamson nanofluid flow across various scenarios demonstrate strong performance in terms of reducing Mean Squared Error (MSE) and achieving high accuracy. In all scenarios, the model exhibited stable convergence with MSE values decreasing significantly throughout the training process, reaching as low as 4.8e-09 in Scenario 4 and 1.2e-07 in Scenario 3. The model consistently showed good generalization, with minimal differences between training, validation, and testing errors, indicating its robustness in solving the complex system of equations governing the fluid dynamics. Performance metrics such as gradient and Mu values remained stable and within acceptable ranges, ensuring efficient training. Overall, the ANN-BLMS model demonstrated effective convergence, accurate predictions, and minimal computational time across all cases, confirming its capability to handle variations in the system parameters with high efficiency and reliability.

4 Conclusion

This study investigates the use of the Artificial Neural Network Backpropagation Levenberg-Marquardt (ANN-BLMS) model to predict the flow characteristics of Casson-Williamson nanofluids under the influence of various physical factors such as magnetic fields, Brownian motion, and thermophoresis. The main findings and contributions of this research are summarized as follows:

- The ANN-BLMS model effectively predicts the velocity, temperature, and concentration profiles of Casson-Williamson nanofluid flow under varying conditions, demonstrating its capability to solve complex nonlinear systems.
- The performance of the ANN model is validated through comparison with numerical results obtained from the bvp4c solver, showing minimal errors and strong generalization for different scenarios.
- The study provides a comprehensive analysis of how the Prandtl number, Weissenberg number, and other fluid parameters affect the nanofluid flow, improving understanding of their roles in heat and mass transfer.
- The Nusselt number (Nu) and Sherwood number (Sh) are evaluated across various scenarios, highlighting how changes in parameters influence heat and mass transfer rates in the nanofluid system, which is critical for optimizing thermal management in engineering applications.
- The results show that the ANN-BLMS model is an efficient tool for rapidly predicting nanofluid behavior, significantly reducing computational time compared to traditional numerical methods.

Data Availability Statement

Data will be made available on request.

Funding

This work was supported without any funding.

Conflicts of Interest

Jagadish V. Tawade served as an Associate Editor of the *ICCK Journal of Applied Mathematics* at the time of manuscript submission. To ensure the integrity of the peer-review process, Jagadish V. Tawade was not involved in the editorial handling, peer review, or decision-making process for this manuscript, which

was handled independently by another editor. The remaining authors declare no conflicts of interest.

Ethical Approval and Consent to Participate

Not applicable.

References

[1] Chamkha, A. J., Rashad, A. M., El-Zahar, E. R., & EL-Mky, H. A. (2019). Analytical and numerical investigation of Fe3O4–water nanofluid flow over a moveable plane in a parallel stream with high suction. *Energies, 12*(1), 198. [Crossref]

[2] Irshad, S., Majeed, A. H., Jahan, S., Riaz, A., Eldin, S. M., & Shahzad, H. (2023). Numerical simulations of MHD generalized Newtonian fluid flow effects on a stretching sheet in the presence of permeable media: A finite difference-based study. *Frontiers in Physics, 11*, 1121954. [Crossref]

[3] Amjad, M., Ahmed, I., Ahmed, K., Alqarni, M. S., Akbar, T., & Muhammad, T. (2022). Numerical solution of magnetized Williamson nanofluid flow over an exponentially stretching permeable surface with temperature dependent viscosity and thermal conductivity. *Nanomaterials, 12*(20), 3661. [Crossref]

[4] Srinivasulu, T., & Goud, B. S. (2021). Effect of inclined magnetic field on flow, heat and mass transfer of Williamson nanofluid over a stretching sheet. *Case Studies in Thermal Engineering, 23*, 100819. [Crossref]

[5] Khader, M. M., Ahmad, H., Adel, M., & Megahed, A. M. (2024). Numerical analysis of the MHD Williamson nanofluid flow over a nonlinear stretching sheet through a Darcy porous medium: Modeling and simulation. *Open Physics, 22*(1), 20240016. [Crossref]

[6] Makhdoum, B. M., Mahmood, Z., Fadhl, B. M., Aldhabani, M. S., Khan, U., & Eldin, S. M. (2023). Significance of entropy generation and nanoparticle aggregation on stagnation point flow of nanofluid over stretching sheet with inclined Lorentz force. *Arabian Journal of Chemistry, 16*(6), 104787. [Crossref]

[7] Kumar, R. M., Raju, R. S., Mebarek-Oudina, F., Kumar, M. A., & Narla, V. K. (2024). Cross-diffusion effects on an MHD Williamson nanofluid flow past a nonlinear stretching sheet immersed in a permeable medium. *Frontiers in Heat and Mass Transfer, 22*(1), 15-34. [Crossref]

[8] Mahmood, Z., Alhazmi, S. E., Alhowaity, A., Marzouki, R., Al-Ansari, N., & Khan, U. (2022). MHD mixed convective stagnation point flow of nanofluid past a permeable stretching sheet with nanoparticles aggregation and thermal stratification. *Scientific Reports, 12*(1), 16020. [Crossref]

[9] Yousef, N. S., Megahed, A. M., Ghoneim, N. I., Elsafi, M., & Fares, E. (2022). Chemical reaction impact on MHD dissipative Casson-Williamson nanofluid flow over a slippery stretching sheet through porous medium. *Alexandria Engineering Journal, 61*(12), 10161-10170. [Crossref]

[10] Bouslimi, J., Omri, M., Mohamed, R. A., Mahmoud, K. H., Abo-Dahab, S. M., & Soliman, M. S. (2021). MHD Williamson nanofluid flow over a stretching sheet through a porous medium under effects of joule heating, nonlinear thermal radiation, heat generation/absorption, and chemical reaction. *Advances in Mathematical Physics, 2021*(1), 9950993. [Crossref]

[11] Panigrahi, L., Panda, J., Swain, K., & Dash, G. C. (2020). Heat and mass transfer of MHD Casson nanofluid flow through a porous medium past a stretching sheet with Newtonian heating and chemical reaction. *Karbala International Journal of Modern Science, 6*(3), 11. [Crossref]

[12] Abbas, A., Jeelani, M. B., Alnahdi, A. S., & Ilyas, A. (2022). MHD Williamson nanofluid fluid flow and heat transfer past a non-linear stretching sheet implanted in a porous medium: effects of heat generation and viscous dissipation. *Processes, 10*(6), 1221. [Crossref]

[13] Tawade, J. V., Guled, C. N., Noeiaghdam, S., Fernandez-Gamiz, U., Govindan, V., & Balamuralitharan, S. (2022). Effects of thermophoresis and Brownian motion for thermal and chemically reacting Casson nanofluid flow over a linearly stretching sheet. *Results in Engineering, 15*, 100448. [Crossref]

[14] Saleem, S., Abbas, T., Abutuqayqah, H., Haq, E. U., & Khan, S. U. (2023). Numerical simulation accompanied by an intelligent computing system for the chemical reaction of Casson nanofluid and radiative heat flux on a nonlinear stretching surface. *Alexandria Engineering Journal, 79*, 629-643. [Crossref]

[15] Alkasasbeh, H. (2022). Numerical solution of heat transfer flow of casson hybrid nanofluid over vertical stretching sheet with magnetic field effect. *CFD Lett, 14*(3), 39-52. [Crossref]

[16] Nasir, S., & Berrouk, A. S. (2023). Numerical and intelligent neuro-computational modelling with Fourier's energy and Fick's mass flux theory of 3D fluid flow through a stretchable surface. *Engineering Applications of Computational Fluid Mechanics, 17*(1), 2270675. [Crossref]

[17] Kumar, P., Nagaraja, B., Almeida, F., AjayKumar, A. R., Al-Mdallal, Q., & Jarad, F. (2023). Magnetic dipole effects on unsteady flow of Casson-Williamson nanofluid propelled by stretching slippery curved melting sheet with buoyancy force. *Scientific Reports, 13*(1), 12770. [Crossref]

[18] Swapna, D., Govardhan, K., Narender, G., & Misra, S. (2023). Viscous dissipation and Chemical reaction on Radiate MHD Casson nanofluid past a stretching surface with a slip effect. *Journal of Heat and Mass Transfer Research, 10*(2), 315-328. [Crossref]

[19] Ullah, A., Yao, H., Waseem, Saboor, A., Awwad, F. A., & Ismail, E. A. (2024). A qualitative analysis of the artificial neural network model and numerical solution for the nanofluid flow through an exponentially stretched surface. *Frontiers in Physics, 12*, 1408933. [Crossref]

[20] Abbas, W., Megahed, A. M., Ibrahim, M. A., & Said, A. A. (2023). Ohmic dissipation impact on flow of Casson-Williamson fluid over a slippery surface through a porous medium. *Indian Journal of Physics, 97*(14), 4277-4283. [Crossref]

[21] Ali, U., Irfan, M., Akbar, N. S., Rehman, K. U., & Shatanawi, W. (2024). Dynamics of Soret–Dufour effects and thermal aspects of Joule heating in multiple slips Casson–Williamson nanofluid. *International Journal of Modern Physics B, 38*(16), 2450206. [Crossref]

[22] Zhu, A., Ali, H., Ishaq, M., Junaid, M. S., Raza, J., & Amjad, M. (2022). Numerical study of heat and mass transfer for Williamson nanofluid over stretching/shrinking sheet along with Brownian and thermophoresis effects. *Energies, 15*(16), 5926. [Crossref]

[23] Khan, K. A., Javed, M. F., Ullah, M. A., & Riaz, M. B. (2023). Heat and mass transport analysis for Williamson MHD nanofluid flow over a stretched sheet. *Results in Physics, 53*, 106873. [Crossref]

[24] Yahya, A. U., Salamat, N., Huang, W. H., Siddique, I., Abdal, S., & Hussain, S. (2021). Thermal charactristics for the flow of Williamson hybrid nanofluid (MoS2+ ZnO) based with engine oil over a streched sheet. *Case Studies in Thermal Engineering, 26*, 101196. [Crossref]

[25] Arshad, M., Hussain, A., Hassan, A., Haider, Q., Ibrahim, A. H., Alqurashi, M. S., ... & Abdussattar, A. (2021). Thermophoresis and brownian effect for chemically reacting magneto-hydrodynamic nanofluid flow across an exponentially stretching sheet. *Energies, 15*(1), 143. [Crossref]

[26] Tedjani, A. H. (2023). Numerical treatment via the spectral collocation method for Casson–Williamson nanofluid flow due to a stretching sheet with slip conditions. *Case Studies in Thermal Engineering, 51*, 103588. [Crossref]

[27] Lone, S. A., Shamshuddin, M. D., Shahab, S., Iftikhar, S., Saeed, A., & Galal, A. M. (2023). Computational analysis of MHD driven bioconvective flow of hybrid Casson nanofluid past a permeable exponential stretching sheet with thermophoresis and Brownian motion effects. *Journal of Magnetism and Magnetic Materials, 580*, 170959. [Crossref]

[28] Zaman, S. U., Aslam, M. N., Riaz, M. B., Akgul, A., & Hussan, A. (2024). Williamson MHD nanofluid flow with radiation effects through slender cylinder. *Results in Engineering, 22*, 101966. [Crossref]

[29] Jawad, M., Saeed, A., Gul, T., & Bariq, A. (2021). MHD Darcy-Forchheimer flow of Casson nanofluid due to a rotating disk with thermal radiation and Arrhenius activation energy. *Journal of Physics Communications, 5*(2), 025008. [Crossref]

[30] Haq, S. U., Ashraf, M. B., & Tanveer, A. (2024). Artificial neural network analysis of natural convection of Casson fluid flow over a curved stretching surface with viscous dissipation. *International Journal of Thermofluids, 24*, 100973. [Crossref]

[31] Prakash, J., Tripathi, D., Bég, O. A., & Srivastava, V. (2022). EMHD Casson hybrid nanofluid flow over an exponentially accelerated rotating porous surface. *Journal of Porous Media, 25*(11). [Crossref]

[32] Venkata Ramudu, A. C., Anantha Kumar, K., Sugunamma, V., & Sandeep, N. (2020). Heat and mass transfer in MHD Casson nanofluid flow past a stretching sheet with thermophoresis and Brownian motion. *Heat Transfer, 49*(8), 5020-5037. [Crossref]

[33] Sharanayya, & Biradar, S. (2023). Magnetized dissipative Casson nanofluid flow over a stretching sheet with heat source/sink and soret effect under porous medium. *BioNanoScience, 13*(4), 2103-2121. [Crossref]

[34] Leng, Y., Li, S., Algarni, S., Jamshed, W., Alqahtani, T., Ibrahim, R. W., ... & Hassan, A. M. (2024). Computational study of magnetized and dual stratified effects on Non-Darcy Casson nanofluid flow: An activation energy analysis. *Case Studies in Thermal Engineering, 53*, 103804. [Crossref]

[35] Ali, A., Ahammad, N. A., Tag-Eldin, E., Gamaoun, F., Daradkeh, Y. I., & Yassen, M. F. (2022). MHD Williamson nanofluid flow in the rheology of thermal radiation, Joule heating, and chemical reaction using the Levenberg–Marquardt neural network algorithm. *Frontiers in Energy Research, 10*, 965603. [Crossref]

[36] Nayak, B., Panda, M., & Mishra, S. R. (2024). Analysis of Brownian motion and thermophoresis effects with chemical reaction on Williamson nanofluid flow over permeable stretching sheet. *Partial Differential Equations in Applied Mathematics, 11*, 100908. [Crossref]

[37] Khan, A., Aljuaydi, F., Khan, Z., & Islam, S. (2024). Numerical analysis of thermophoretic particle deposition on 3D Casson nanofluid: artificial neural networks-based Levenberg–Marquardt algorithm. *Open Physics, 22*(1), 20230181. [Crossref]

[38] Ramasekhar, G., Alkarni, S., & Shah, N. A. (2024). Machine learning approach of Casson hybrid nanofluid flow over a heated stretching surface. *AIMS Mathematics, 9*(7), 18746-18762. [Crossref]

[39] Srinivasacharya, D., & Kumar, R. S. (2022). Artificial neural network modeling of the Casson fluid flow over unsteady radially stretching sheet with Soret and Dufour effects: D. Srinivasacharya, RS Kumar. *Journal of Thermal Analysis and Calorimetry, 147*(24), 14891-14903. [Crossref]